buildings

MDPI

Article

Analytical and Numerical Evaluation of Additional Deflection in Tapered Steel Beams with Variable Diameter Web Openings

Amine Osmani [1,*], Amine Zemri [2], Abdelwahhab Khatir [1] and Si Fodil Djamel [3]

[1] LM2SC, Civil Engineering Department, University of Science and Technology of Oran Mohamed Boudiaf (USTO-MB), 1505, EL MNAOUER, Oran 31000, Algeria; abdelwahhab.khatir@univ-usto.dz
[2] Civil Engineering and Public Works Department, University of Relizane, Relizane 48000, Algeria; amine.btp@hotmail.fr
[3] LMST, Civil Engineering Department, University of Science and Technology of Oran Mohamed Boudiaf (USTO-MB), 1505, EL MNAOUER, Oran 31000, Algeria; djamel.sifoudil@univ-usto.dz
* Correspondence: amine.osmani@univ-usto.dz

Abstract

This study presents an analytical formulation for predicting the additional elastic deflection of tapered steel beams with variable-diameter circular web openings, a configuration that is not addressed by existing analytical models or current design codes. The proposed formulation accounts for the coupled effects of cross-section tapering, progressive variation in opening diameter along the span, and shear–bending interaction within perforated regions. To the best of the authors' knowledge, this is the first analytical model addressing such complex non-prismatic cellular beam configurations. The formulation is implemented in MATLAB R2019a, enabling fast and automated deflection calculations over a wide parametric range, including various loading cases, tapering ratios, beam spans, web-post widths, and opening dimensions. For prismatic configurations, the analytical predictions are benchmarked against Eurocode 3 and the SCI P355 design guide, both originally developed for beams with constant cross-sections and regular openings. The results demonstrate the improved accuracy and broader applicability of the proposed approach. For tapered configurations with variable-diameter openings, the formulation is assessed against finite element simulations performed in Abaqus/CAE 2017, with the numerical model previously validated against experimental results available in the literature. The proposed method provides a reliable and practical analytical tool for the serviceability assessment of tapered perforated steel beams in structural engineering applications.

Keywords: tapered steel beams; cellular beams; variable-diameter web openings; additional deflection; analytical model

Check for updates

Academic Editor: Jingzhong Tong

Received: 6 February 2026
Revised: 20 March 2026
Accepted: 26 March 2026
Published: 30 March 2026

Copyright: © 2026 by the authors. Licensee MDPI, Basel, Switzerland. This article is an open access article distributed under the terms and conditions of the Creative Commons Attribution (CC BY) license.

1. Introduction

The standard elements with web openings, such as cellular and castellated beams, are steel I-section profiles with regularly spaced circular or hexagonal openings in the web. Their ability to provide long, unobstructed spans makes them highly attractive in modern construction (Figure 1a). To meet increasing performance and efficiency demands, engineers have explored innovative geometries. One such development is the cellular tapered steel beam with variable-diameter openings (Figure 1d). In addition to the advantages of conventional cellular beams, tapered beams optimise material use by reducing cross-sections in low-stress regions, producing lighter and more efficient structures.

However, these benefits require careful consideration of the combined effects of tapering and web openings, both of which significantly influence serviceability performance, particularly deflections.

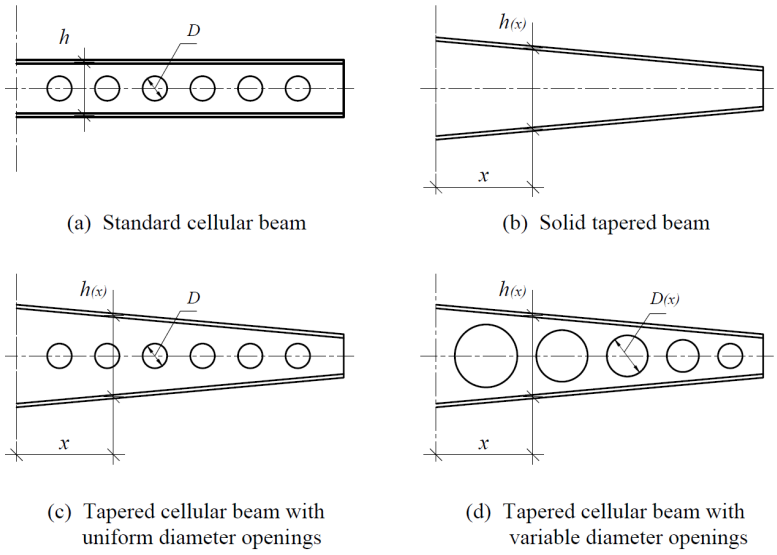


Figure 1. Evolution of cellular steel beam.

Deflection evaluation for perforated beams has traditionally relied on semi-empirical solutions in Eurocode 3 [1] and the British guide SCI P355 [2]. Both are based on reduction factors (EC3) or simplified coefficients (SCI P355), but they remain limited, particularly for beams with large diameter-to-depth ratios or closely spaced openings. Regarding tapered steel beams, existing investigations have focused primarily on stability and resistance, with deflection assessment relying exclusively on numerical approaches. No analytical or semi-analytical formulation has been established for such members, whether for solid-web or perforated configurations, which further highlights the gap addressed in the present study. Osmani et al. [3] advanced the field by developing an analytical model for non-prismatic beams with constant-diameter openings (Figure 1c). However, this model is strictly limited to regularly spaced openings of uniform diameter and does not incorporate the progressive geometric variation in perforations along the beam span. As demonstrated in the parametric study (Section 4), the variation in opening diameter along the span has a significant influence on the additional deflection, particularly for short spans and low tapering ratios (α = 0.4). In tapered beams with variable openings, local deformations around perforations are amplified due to the reduced stiffness of the T-shaped sections and must be properly addressed for reliable serviceability checks. Yet, current analytical approaches and design codes provide no tools for such configurations. An extensive review of the available literature confirms that no analytical, semi-analytical, or empirical formulation has been proposed for the deflection of tapered steel beams with variable-diameter web openings. Existing models, including those in EC3, SCI P355, and recent works such as Osmani et al. [3], are restricted to either prismatic beams or tapered beams with constant-diameter openings. The present work is, to the best of the authors' knowledge, the first to address this combined configuration analytically.

This paper addresses this gap by presenting a new analytical formulation to predict the additional deflection of such beams. The method integrates the effects of tapering, variable opening size, and combined shear–bending deformation. It covers a wide parameter range relevant to practice and is implemented in MATLAB R2019a for fast and automated calculations, making it suitable for both engineering use and structural software environments.

Steel beams with web openings were first used in Europe in the 1940s, initially with hexagonal perforations [4]. Circular web openings appeared in the 1980s in projects such as Chicago O'Hare Airport (Figure 2). Since Horton's 1910s proposal of castellated beams as cited in Das & Seimaini [5], perforated beams have become widespread in construction, aerospace, and shipbuilding, valued for their high strength-to-weight ratio [6]. Large openings, however, introduce complex behaviours and additional failure modes [7]. Research has identified six principal modes [8–10], with the Vierendeel mechanism (VM) and web post buckling (WPB) being dominant in beams with closely spaced openings. VM was first observed in castellated beams by Altifillisch et al. [8], then in cellular beams by Redwood et al. [9]. Kerdal and Nethercot [10] showed experimentally that VM is strongly influenced by web thickness and opening diameter. Other key phenomena include lateral torsional buckling (LTB) and WPB. Aglan and Redwood [11] predicted WPB loads from shear using finite differences, proposing design approximations for various geometries. More recently, refs. [12–14] explained LTB in cellular beams as arising from insufficient lateral support of the compressed tee, with torsional effects resisted by the web. Numerous studies have confirmed that perforated profiles share failure modes with castellated and cellular beams [15]. In 2010, Tsavdaridis pioneered beams with elliptical openings [16], later patented [17]. These provide a cost-effective alternative with promising structural behaviour. Subsequent studies proposed equations for WPB resistance [18] and optimisation of opening shapes [18–21]. Parallel work on tapered members has produced experimental and analytical results [22–28], confirming that they also experience instability modes similar to prismatic beams. The patch loading performance of plate girders with web openings has also been recently investigated, highlighting the significant influence of opening size on ultimate resistance [29].



Figure 2. Real-world application of tapered cellular steel beams in a building structure [30].

This paper, however, focuses on serviceability, specifically deflection. Web openings reduce local stiffness and increase overall deflections. Gibson et al. [31] were among the first to investigate deflections in castellated beams, proposing an approximate method based on the Vierendeel analogy, which showed good agreement with tests. Later, Iverson et al. [32] and Hosain et al. [33] used finite element methods, while Lawson [34] introduced analytical formulations for beams with single openings. He showed that perforated beams deflect only about 5% more than equivalent solid beams. Chung and Lawson [35] proposed design rules for composite beams with continuous openings, estimating additional deflection with a

simple factor. Lawson et al. [36] further simplified this, accounting for large or asymmetric openings, with an additional 33% increase due to shear effects. Liu and Chung [37] derived an equation including Vierendeel bending, shear, and axial deformation of the tees, with results incorporated into BS 5950 [38]. Warren [39] used Euler–Bernoulli theory but neglected shear strain, limiting the method to unperforated beams. Djebli et al. [40,41] refined models to include shear deformation and Vierendeel bending, showing that shorter beams experience proportionally greater additional deflection. More recently, Osmani et al. [3] developed a formulation that matched finite element results for both prismatic and non-prismatic cellular beams, while exposing significant inaccuracies in SCI P355 predictions. However, this model remains unsuitable for beams with variable-diameter openings. More recently, machine learning-based approaches have also been explored for perforated steel members, offering new perspectives on resistance prediction and web crippling behaviour of perforated sections [42,43].

In response, this paper introduces a refined analytical formulation that incorporates both tapering and gradual opening variation, accounting for interactions between shear and bending in perforated regions. The approach accurately predicts the additional deflection from non-uniform perforations, an aspect neglected in conventional methods and design codes. Implemented in MATLAB R2019a, the algorithm enables fast and automated analytical calculation of the additional deflection w_{add} across a variety of beam types and load cases. The baseline deflection w_0 of the unperforated tapered beam, for which no closed-form solution exists, can be independently computed using any standard structural analysis software, and combined with w_{add} to obtain the total deflection w. Analytical results are benchmarked against Eurocode 3, SCI P355, and finite element simulations in Abaqus/CAE2017, with further validation against experimental data. This multi-level comparison confirms both the accuracy and practical relevance of the proposed approach.

2. Analytical Approach

To undertake the deflections analysis of non-prismatic perforated web elements with VDOs, the simply supported beam loaded in three points, four points and five points bending, and the cantilever beams subjected to concentrated load at the free end are considered in this paper. A straight tapered cellular steel beam with VDOs, along with labelled dimensions used in this study, is pictured in Figure 3.

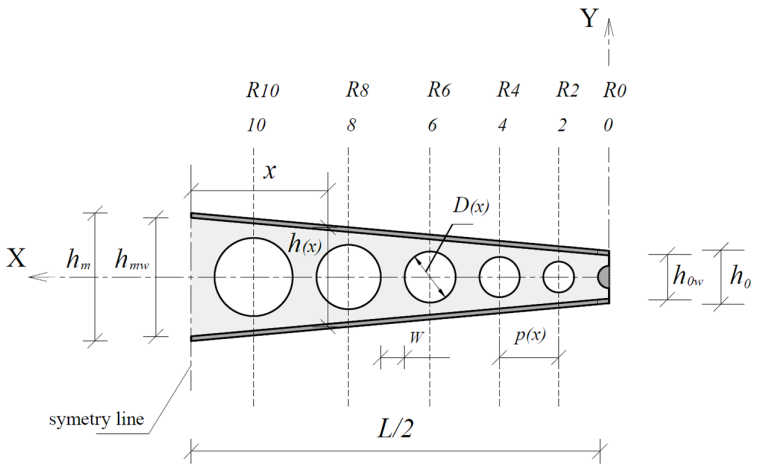


Figure 3. Geometrical properties of a tapered I-section beam with VDOs in the web.

The maximum deflection calculated at mid span w is decomposed into two terms, w_0 corresponding to the unperforated tapered beam deflection and w_{add} corresponding to the additional deflection due to the existence of openings in the web.

$$w = w_0 + w_{add} \tag{1}$$

Since there is not yet an expression that evaluates the deflection of unperforated beams with tapered sections, w_0 is calculated according to the Euler–Bernoulli numerical finite element model, developed for the four load cases and for different tapered web section parameters. This numerical computation does not affect the analytical nature of the proposed formulation, whose original contribution resides entirely in the analytical evaluation of w_{add}.

The additional deflection is evaluated under transversal load according to the Vierendeel effect; it is an addition to the shear displacement w_{Ts} and bending displacements w_{Tb} which are taken into account at each circular web opening of the top and bottom T-sections. These local deflections are influenced by the tapered geometry of the beam, with the parameter (α) representing the variation in web height (Equation (2)).

$$\alpha = \frac{h_{min}}{h_{max}} \tag{2}$$

In this expression, h_{max} denotes the vertical distance between the outer edges of the upper and lower flanges at the beam's mid-span $x = L/2$, whereas h_{min} corresponds to this same distance measured at the beam supports at $x = 0$ and $x = L$.

We assume that the displacement of the upper and lower T-sections has the same value, because this analysis is only for the symmetric cross-section. In this paper, the asymmetric cross-section is not considered; thus, the two T-sections have the same shear and bending strains. However, each T-section has a displacement w_t as shown in Figure 4.

$$w_t = w_{Tb} + w_{Ts} \tag{3}$$

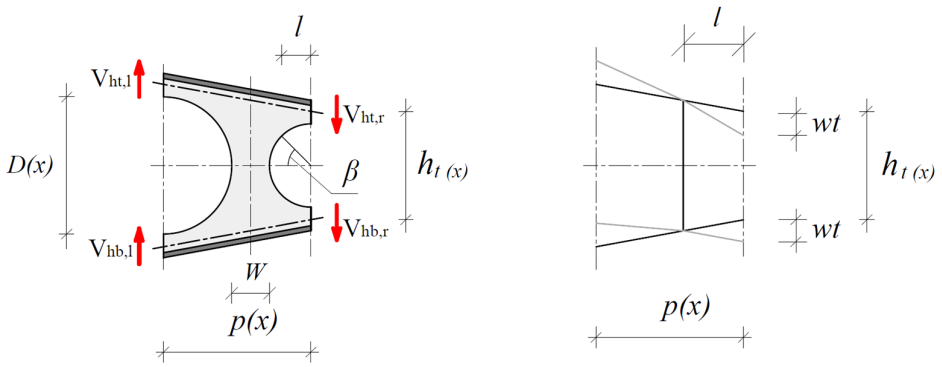


Figure 4. Tapered I-section cellular beam under transverse loading.

The deflection under the bending effect of the top and bottom T-sections is given by the following expression:

$$w_{Tb} = \frac{V\, l^3}{3\, E\, i_w} \tag{4}$$

$$i_f = \frac{b_f\, {t_f}^3}{12} \tag{5}$$

$$i_w = \frac{t_w \left(\frac{h_w(x) - D(x)}{2}\right)^3}{12} \tag{6}$$

$$i_T = i_f + A_f \cdot d_f^2 + i_w + A_w(x) \cdot d_w^2(x) \tag{7}$$

i_f, i_w and i_T are the moments of inertia of the flange, the web of the T-section and the entire T-section, respectively. A_f denotes the area of the flange, d_f denotes the distance between the centroid of the I-section and the centroid of the flange section, $A_w(x)$ denotes the area of the tapered web of the T-section, and $d_w(x)$ denotes the distance between the centroid of the I-section and the centroid of the web-tapered T-section. The value of the angle β is fixed to 45°, adopted as the equivalent rectangular shape to comply with current European and UK guidelines (EC3 and SCI P355). This assumption is commonly used when circular openings are approximated as equivalent rectangular shapes, in order to simplify the description of the stress field around the opening. Previous studies reported by Lawson [36] and Tsavdaridis [16] have shown that the angle β varies between 25 and 40 degrees for perforated beams with circular web openings, depending on the shear–moment ratio applied at the centreline of the openings. The Vierendeel effect is generally dominant for openings with a large length under high shear force, whereas for circular openings its influence is less pronounced [44]. The angle β represents the local plasticization of the section around the circular opening. This value has also been previously adopted and validated in an earlier study [3], where analytical predictions showed good agreement with finite element simulations, confirming that $\beta = 45°$ provides a reasonable approximation for circular web openings. According to the Vierendeel mechanism, the upper and the lower T-sections behave as a cantilever beam subjected to external shear load V, whose length l is calculated in Equation (8).

$$l(x) = R(x)\, sin\beta \tag{8}$$

where

$R(x)$ is the radius of the circular opening in the web.

The deflection under the shear effect of the upper and lower T-sections is given by the following expressions:

$$w_{Ts} = \frac{V\, l(x)}{G\, \omega(x)} \tag{9}$$

$$G = \frac{E}{2 \cdot (1 + v)} \tag{10}$$

$$\omega(x) = \frac{(h_w(x) - 2R(x))}{2} \cdot t_w \tag{11}$$

$$h_w(x) = h(x) - 2\, t_f \tag{12}$$

The total additional deflection $w_{add\ i}$ at one opening of the cellular beam is given by Equation (13), i corresponding to the position of the opening number on the cellular beam:

$$w_{add\ i} = 2\, w_t \tag{13}$$

At the end, the expression Equation (14) presents the additional deflection of n-openings, for the tapered steel beams with several openings with VDOs:

$$w_{add} = \sum_{i=0}^{m} w_{add\ i} \tag{14}$$

As mentioned in Figure 3, the opening circular diameters D are not constant along the beam axis, and they depend on the height of its cross-section at the coordinate x, as well as on the ratio ρ (Equation (17)). For this task, and to be able to calculate the additional deflection of the tapered cellular steel beam with VDOs, an algorithm has been developed by MATLAB R2019a [45]. It can provide the deflection of any geometry of the elements studied for "n" openings, different tapered section parameters α, variable diameter along the beam, and the load cases treated in this paper. The algorithm is built with a loop whose counter is parameterized by the index i and starts from 2 up to with $m = 2 \times n$.

The expressions used in the algorithm are presented in the following expressions:

$$x_i = R_0 + \frac{i}{2}W + R_0 \left(\sum_{j=0}^{\frac{i}{2}-1} 2\,\psi^j + \psi^{\frac{i}{2}} \right) \tag{15}$$

$$h(x) = \left(\frac{2 \cdot (h_m - h_0)}{L} \right) \cdot x + h_0 \tag{16}$$

$$D(x) = \rho \cdot h(x) \tag{17}$$

Equation (15) represents a key advancement in this analytical framework, as it defines the exact longitudinal position x of each circular web opening along the tapered beam, taking into account the progressive variation in their diameters. This equation was not part of the earlier formulation developed in Osmani et al. [3], which was limited to constant-diameter and regularly spaced openings. Its inclusion in the present study allows for a more realistic modelling of variable perforation patterns, as commonly encountered in optimised structural systems. Coupled with Equations (16) and (17), this formulation enables the definition of each opening's diameter as a function of its position along the beam, while maintaining a constant D_x/h_x ratio. This geometric consistency is critical for evaluating stiffness loss in the perforated regions. Moreover, the expression guarantees a uniform web-post spacing W, ensuring accurate modelling of intermediate openings and their structural influence. As such, Equation (15) serves as a fundamental component in achieving both analytical precision and computational efficiency in the implemented algorithm. The derivation of Equation (15) is based on the geometric consistency condition that the ratio $D(x)/h(x) = \rho$ must remain constant along the beam span. This requires that the radii of successive openings form a geometric sequence of ratio $\psi = R_i/R_{i-2}$, giving $R_2 = \psi R_0$, $R_4 = \psi^2 R_0$, …, $R_i = \psi^{(i/2)} R_0$. The longitudinal position of each opening is obtained by cumulating the radii and web-post widths. Developing case by case and generalising for even index i yields Equation (15). The summation term $2\sum \psi^j$ represents the cumulative contribution of all preceding opening radii to the position of the current opening, while $\psi^{\frac{i}{2}}$ corresponds to the radius of the current opening itself.

3. Finite Element Modelling

3.1. Validation of Finite Element Model

To validate the proposed method for analysing deflection in tapered cellular steel beams with variable-diameter openings in the web, we conduct a comparative assessment. A three-dimensional finite element model was developed using Abaqus/CAE2017 [46] to perform both geometrical and material nonlinear analyses. To validate the model, the experimental results of tests A2, A5, A6, B1, B5, and B6 conducted by Grilo et al. [47] on prismatic steel cellular beams were used. The geometric properties of the tested specimens are detailed in Table 1. The numerical analysis is carried out in two stages: buckling followed by post-buckling analysis. This approach has previously been adopted in studies [48–50]. In

the post-buckling phase, a geometrically and materially nonlinear analysis including imperfections (GMNIA) is conducted, incorporating initial imperfections through the use of the *IMPERFECTION command. The initial geometric imperfection values were adopted from the numerical model of Grilo et al. [47], which was validated against their experimental results. The good agreement between the simulated and experimental load–displacement curves confirms the appropriateness of the adopted imperfection values. To guarantee the reliability of the analysis, the I-sections were discretized using S4R shell elements (four-node quadrilateral elements with reduced integration), with a mesh size of 10 mm. A mesh sensitivity study was conducted in refs. [48,49], comparing different mesh sizes and confirming that the 10 mm mesh provides converged and mesh-independent results for this type of configuration. This discretization was therefore adopted in the present work to ensure accurate and reliable finite element results across all the cellular beams investigated. The S4R shell element, characterised by its six degrees of freedom (three translational and three rotational), was selected due to its capability to deliver accurate results while minimising computational cost. The material characteristics of the steel beams are as follows: 0.3 for Poisson's coefficient, 200 GPa for the modulus of elasticity. Residual stresses were not included in the model, as the present study focuses exclusively on elastic deflection. In the elastic range, residual stresses have a negligible influence on deflection behaviour and their inclusion is therefore not required for this type of analysis. The yield and ultimate stress values for each specimen are shown in Table 1.

Table 1. Geometries of cellular steel beams used in validation.

Specimen	t_w	t_f	b_f	s	H	L	D_0	s_0	δ_w	f_y	f_u
A2	4.8	5.6	102	445.8	433	1874	342.5	103.3	2.5	416	480
A5	4.8	6	102	325.1	409	1370	248.8	76.3	8	416	480
A6	4.9	5.8	103	350.1	407	1493	250	100.1	3.5	397	495
B1	5.8	9.1	99	403	442	1642	351.8	51.2	2	398	511
B5	5.9	9	99	318.4	412	1346	243.8	74.6	7.2	398	511
B6	6	9.2	98	343	409	1459	245	98	4.5	398	511

Simply supported beams are considered for all models with lateral restraint at the supports. At one end, at the bottom of the stiffener, transversal and longitudinal displacements are restrained ($U_x = U_y = U_z = 0$), and at the other end, only the transversal displacements are restrained ($U_y = U_z = 0$). Four points were restrained for lateral displacement and the rotation around the longitudinal axis in the region of the stiffeners ($U_z = UR_x = 0$) [51,52], (Figure 5).

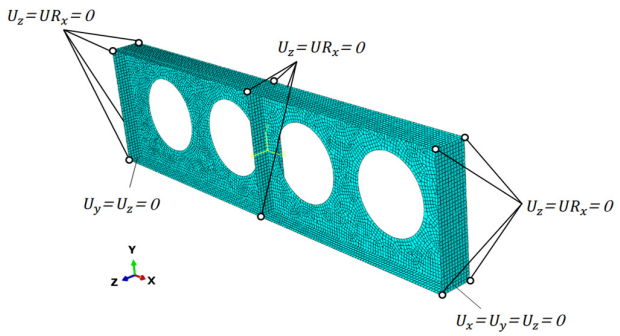


Figure 5. Boundary conditions.

The validation results, shown in Figure 6, focus on the load–displacement relationship for the studied specimens. Based on the illustrations, the numerical model can be considered validated. Since no experimental, numerical, or analytical data exist in the open literature for tapered beams with variable-diameter web openings, the validated FEM model is used as the reference solution for the parametric study presented in Section 4.

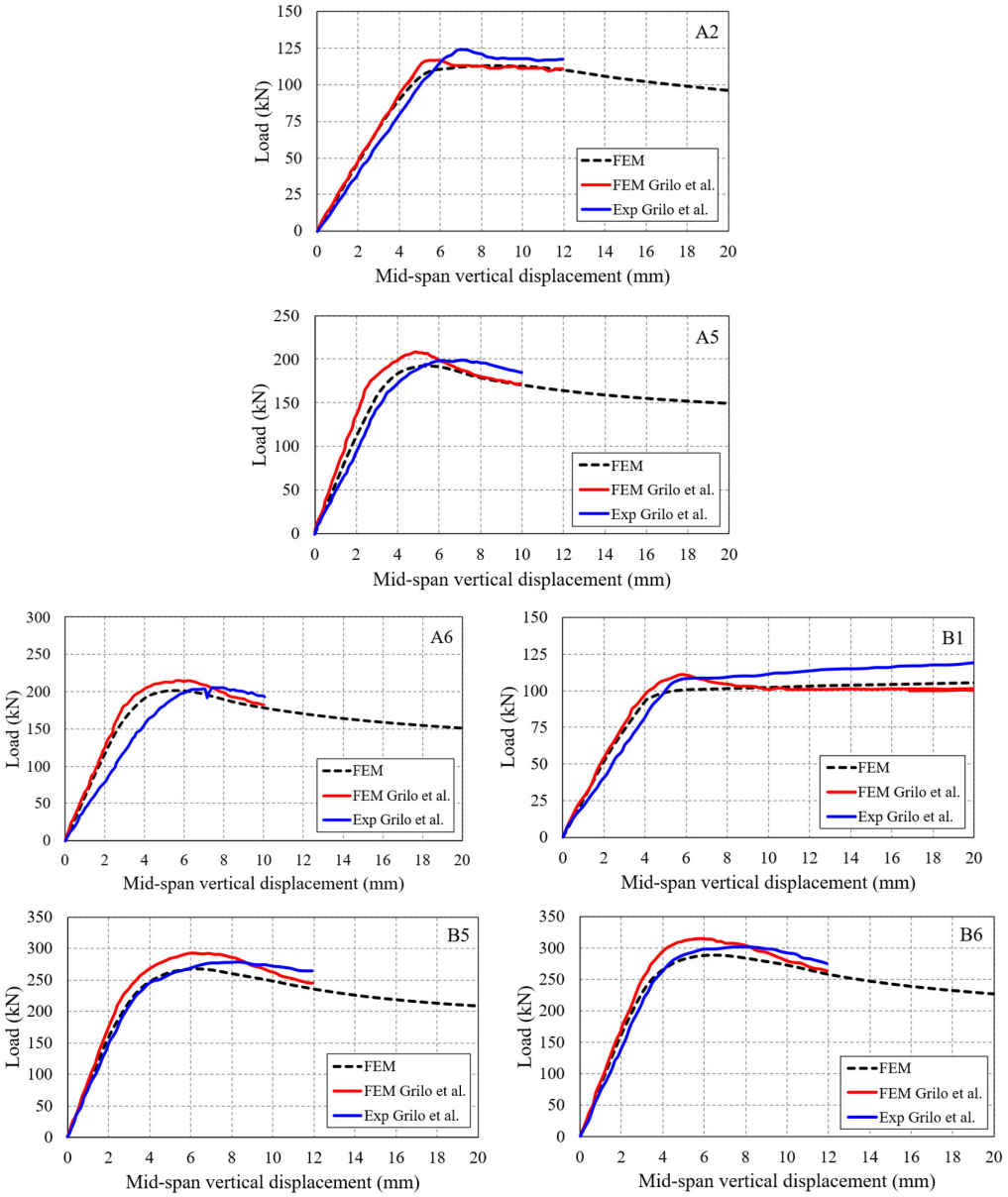


Figure 6. Comparison between test and finite element models by load–displacement relationships [47].

3.2. Benchmarking of the Proposed Analytical Solution Against Fem and Literature (Prismatic Beams Case)

Building on the FEM validation established in the previous section, we perform a comprehensive three-way comparative analysis between: (i) our original analytical solution, (ii) the approximate approach of Eurocode 3, and (iii) the semi-empirical formulations of the UK design guidance SCI P355. It is worth emphasising that the analytical formulation developed in this study is, to the best of our knowledge, the only existing model that simultaneously incorporates both the longitudinal variation in the beam's cross-section ($\alpha \neq 1$) and the variation in the diameter of circular web openings. These two geometric

aspects, though critical to the structural behaviour, have never been jointly addressed in any existing deflection prediction approach. In contrast, the EC3 and SCI P355 formulations are strictly limited to prismatic beams ($\alpha = 1$) with regularly spaced openings of constant-diameter. To ensure a consistent comparison with prismatic beams, we keep tapered parameters fixed to ($\alpha = 1$). The elastic mechanical properties of the steel used in this study are 210 GPa for the modulus of elasticity and 0.3 for Poisson's ratio, respectively.

In this section, only the simply supported beams are considered under three load cases (three-point bending, four-point bending and uniformly distributed load). The additional deflection w_{add} expression adopted by EC3 for multiple regular cellular openings is approximately estimated by the following formula:

$$\frac{\delta_{add}}{\delta_b} = 0.5 \cdot n_0 \cdot k_0 \frac{a_0}{L} \frac{h_0}{h} \tag{18}$$

where:

n_0: Number of regular openings along the beam.

k_0: Correction factor with the following values.

k_0 = 2.0 for an unreinforced opening.

k_0 = 1.5 for a reinforced opening.

a_0: Opening width.

h_0: Opening height.

h: Beam height.

L: Beam span.

w_b: Unperforated beam.

The additional deflection expression adopted by SCI-P355 for multiple regular cellular openings is:

$$\frac{w_{add}}{w_b} = 0.47 \cdot n_0 \cdot k_0 \left(\frac{h_0}{h}\right)^2 \left(\frac{h}{L}\right) \tag{19}$$

where:

n_0: Number of regular openings along the beam.

k_0: Coefficient equal to 1.0 for longitudinally stiffened and 1.5 for unstiffened openings.

h_0: Opening height.

h: Beam height.

L: Beam span.

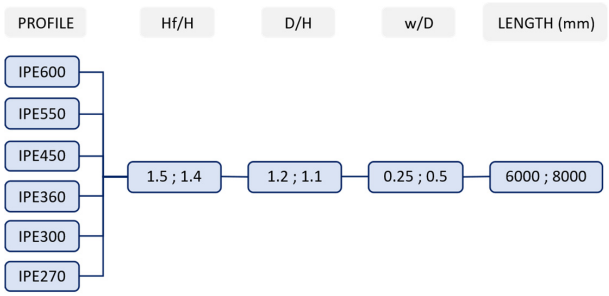
w_b: Unperforated beam.

Figure 7 presents a schematic representation of all models based on ACB manufacturing process configurations, used for the deflection comparison between the analytical method, EC3, and SCI P355, applied to a prismatic cellular steel beam under a three-point bending load. The errors in total deflection values of the proposed method, the EC3, and the SCI P355 approximated approaches compared to the FEM results are presented in Figures 8 and 9. The relative errors associated with the proposed method w, w_{EC3} and $w_{SCI\ P355}$ are defined according to the following expressions:

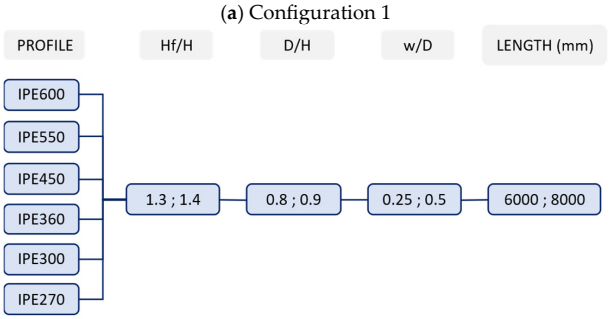
$$\Delta_1 = 100 \times \frac{|w - w_{FEM}|}{w_{FEM}} \tag{20}$$

$$\Delta_2 = 100 \times \frac{|w_{EC3} - w_{FEM}|}{w_{FEM}} \tag{21}$$

$$\Delta_3 = 100 \times \frac{|w_{SCI\ P355} - w_{FEM}|}{w_{FEM}} \tag{22}$$

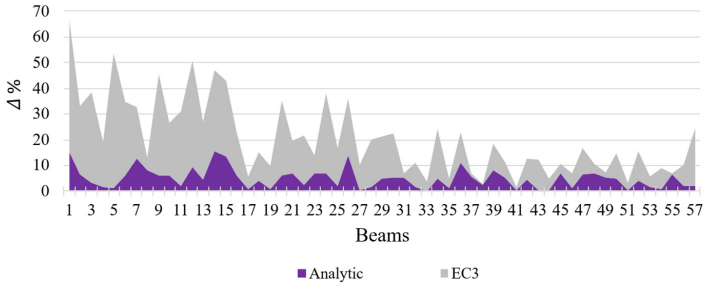


(**a**) Configuration 1

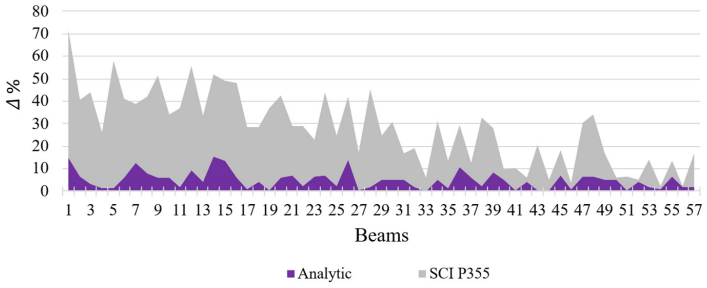


(**b**) Configuration 2

Figure 7. Parameters of numerical models analysed in the benchmark.



(**a**)



(**b**)

Figure 8. Comparison of deflection prediction errors for the first configuration between the proposed analytical method and codes: (**a**) EC 3, (**b**) SCI P355.

Figures 8 and 9 present the results obtained for the two geometric configurations of prismatic cellular beams. In both cases, the proposed analytical method consistently outperforms existing approaches in terms of deflection prediction accuracy, regardless of the beam geometry. Across a wide range of beam cases analysed, the discrepancies between the proposed method and the finite element method (FEM) results remain generally small, often below 10%, and in several instances below 2%. For Configuration 1 (Figure 8), the analytical method shows an average error of 4.7%, compared to 16.9% for the EC3 code and 21.9% for the SCI P355 guide, with peak deviations exceeding 50% for these standard-based methods. Configuration 2 (Figure 9) follows a similar trend, with a slightly higher average error for the proposed method (6.2%), still significantly lower than those of EC3 (14.5%)

and SCI P355 (16.8%). These recurring discrepancies highlight the limitations of normative approaches, which, while useful for general assessments, introduce overly conservative safety margins, particularly in cases involving large openings (Configuration 1). Moreover, the low error dispersion associated with the analytical method (standard deviation < 4% in both configurations) confirms its robustness, whereas the significantly higher variability in the standard-based methods (standard deviation > 10%) underscores their sensitivity to geometric variations. Notable errors are observed for larger cross-sections (IPE 600 to 450) when using EC3 and SCI P355, indicating their limited accuracy in such cases. In contrast, smaller sections (IPE 360 to 270) show a significant reduction in discrepancies, particularly with the analytical method, which remains stable and highly accurate across all studied cases. These findings clearly demonstrate the shortcomings of current EC3 and SCI P355 formulations, which were originally developed for cellular beams with constant cross-sections and regular openings. As a result, they fail to accurately account for the effects of optimised geometries and local deformation mechanisms. The reliance on correction factors or empirical adjustments, as seen in EC3, does not adequately capture the real structural behaviour of such complex systems. In contrast, the proposed analytical model explicitly considers the local displacements of each T-section, incorporating their local stiffness based on the applied forces at their respective positions. This enables a more accurate and consistent prediction of additional deflection, while also offering greater adaptability to a broader range of geometric configurations. This not only confirms the robustness of the developed approach but also demonstrates its practical relevance in scenarios where the simplifying assumptions of existing design codes fall short.

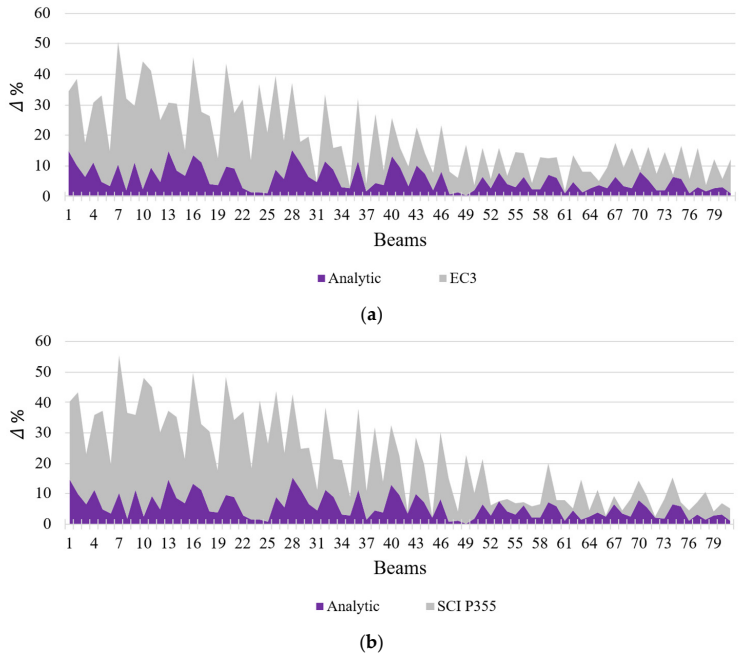


Figure 9. Comparison of deflection prediction errors for the second configuration between the proposed analytical method and codes: (**a**) EC 3, (**b**) SCI P355.

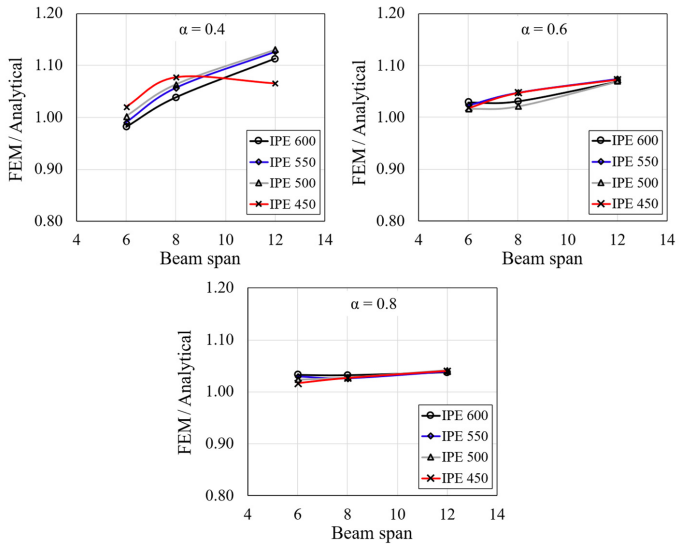
4. Parametric Study

4.1. Comparative Assessment of Analytical and Fem Results: Case of Tapered Beams with Variable-Diameter Web Openings

The FEM validation (Section 3.1) enables reliable parametric analysis of complex geometries where experimental data is unavailable, particularly for: extreme taper cases ($\alpha < 0.5$) and non-linear circular opening arrangements. Four typical steel sections are used in this part, as IPE600, IPE550, IPE500 and IPE450, for three beam span values L (6 m, 8 m,

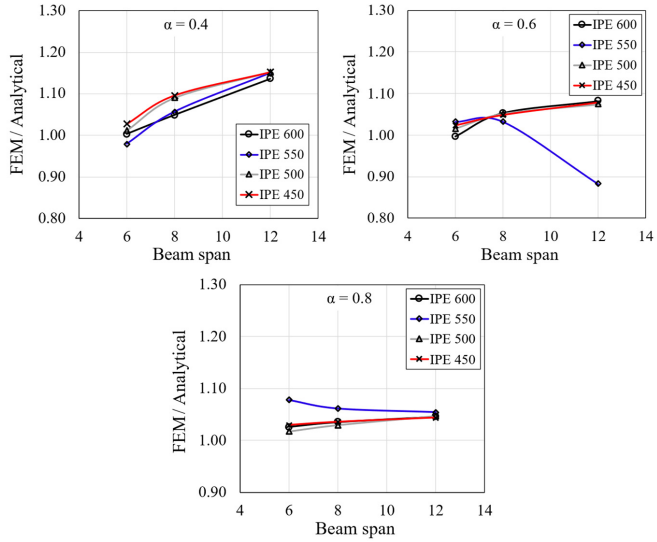
12 m). The diameter ratio of the circular opening along the tapered beam axis is $\rho = 0.8$ of the total height of the beam. The web post has been kept constant. The studied cellular beams do not feature an opening at mid-span. The simply supported beams are used as boundary conditions for the parametric study. The examined beams are subjected to four distinct load cases: three-point bending, four-point bending, five-point bending and beams under uniformly distributed load. The parameter values for the tapered sections under investigation are set at α = 0.4, 0.6 and 0.8. This signifies that at their mid-span, the beams maintain the total height of a typical steel section ($\alpha \neq 1$).

Figure 10 demonstrates a strong correlation between the proposed analytical method and the finite element simulations across all investigated configurations. For the majority of configurations, the ratio of FEM to analytical deflections shows good agreement, with values predominantly close to unity. For three-point and four-point bending cases, deviations remain generally within an acceptable range. However, for five-point bending and uniformly distributed load cases with highly tapered beams (α = 0.4), larger deviations are observed for a limited number of cases. These configurations represent the boundary cases of the parametric range, where the combined effect of strong geometric variation and complex load distribution amplifies local deformations beyond the typical accuracy range of the proposed formulation. The method exhibits consistent accuracy for the majority of configurations, particularly for α = 0.6 and α = 0.8, where results remain close to unity. For highly tapered beams (α = 0.4), larger deviations are observed under five-point bending and uniformly distributed load, representing the boundary cases of the parametric range investigated. The influence of the section variation parameter α is clearly discernible; configurations with α = 0.6 yield the lowest average deviation (2.8%), in contrast to 3.5% for α = 0.4 and 3.2% for α = 0.8. Among the beam profiles, the IPE500 and IPE550 sections consistently produce the best agreement with the FEM data, with mean deviations of 2.9% and 3.1%, respectively, compared to 3.7% for the IPE450 section. These relatively minor discrepancies, coupled with the overall coherence of the response curves, underscore the robustness and reliability of the proposed formulation for predicting the deflection of non-prismatic cellular beams with variable-depth openings. Moreover, the residual deviations exhibit consistent and interpretable patterns, such as a gradual increase with span length and a slight tendency towards overestimation in beams with α = 0.8, suggesting the potential for further refinement through targeted corrective adjustments in future iterations.

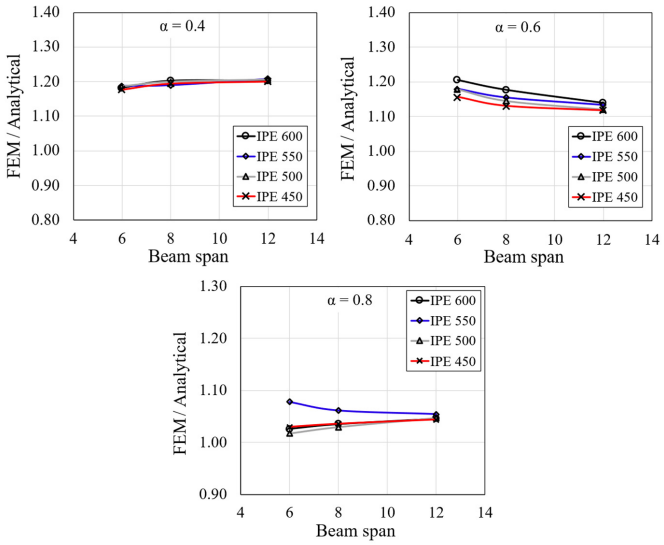


(**a**) Three-point bending

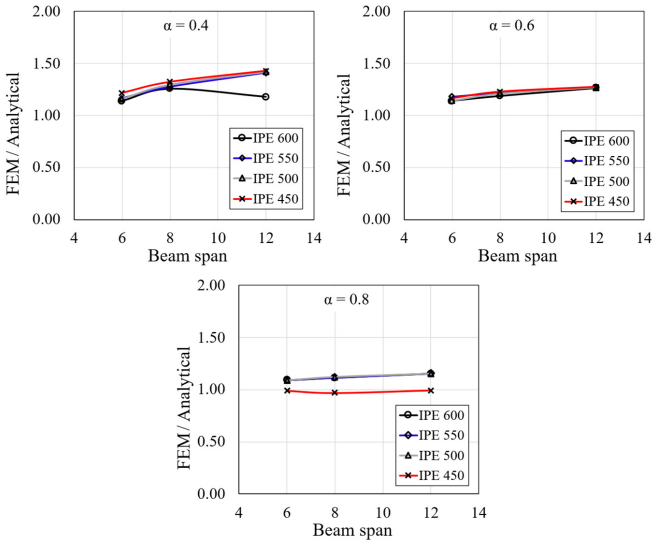
Figure 10. *Cont.*



(**b**) Four-point bending



(**c**) Five-point bending

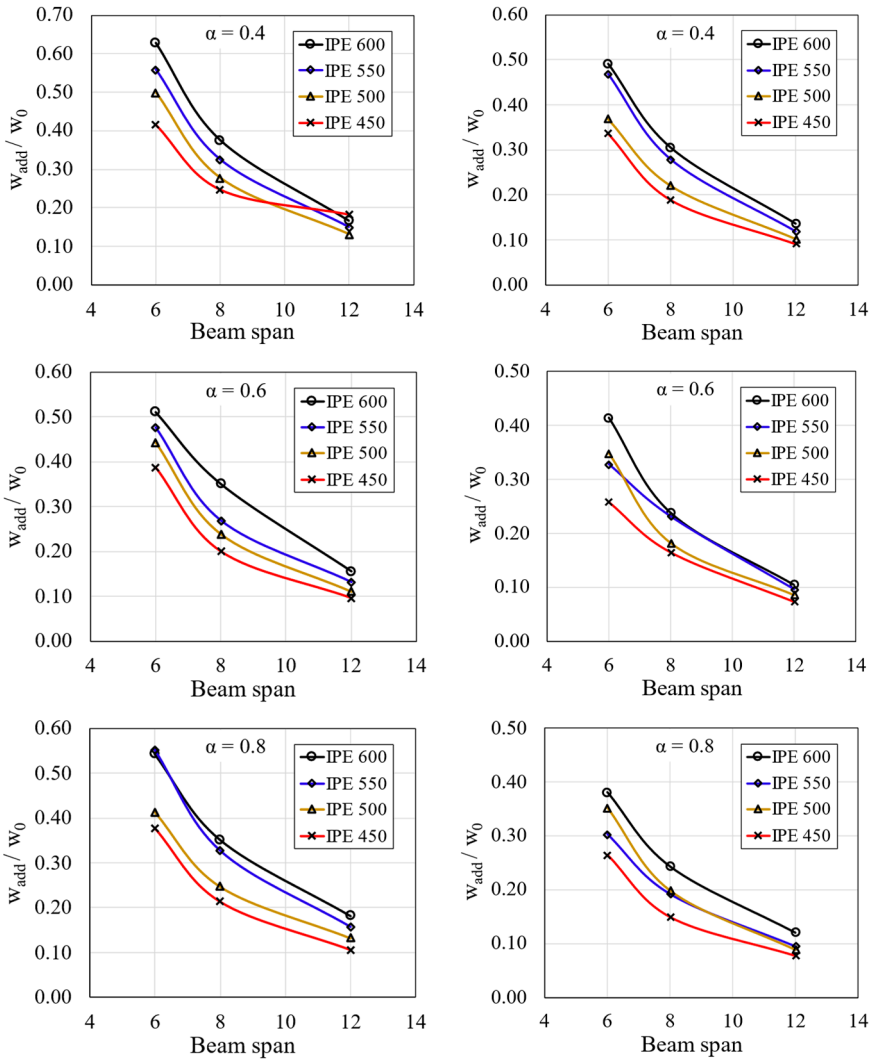


(**d**) Uniformly distributed load

Figure 10. Deflection ratios (FEM/Analytical) versus beam spans.

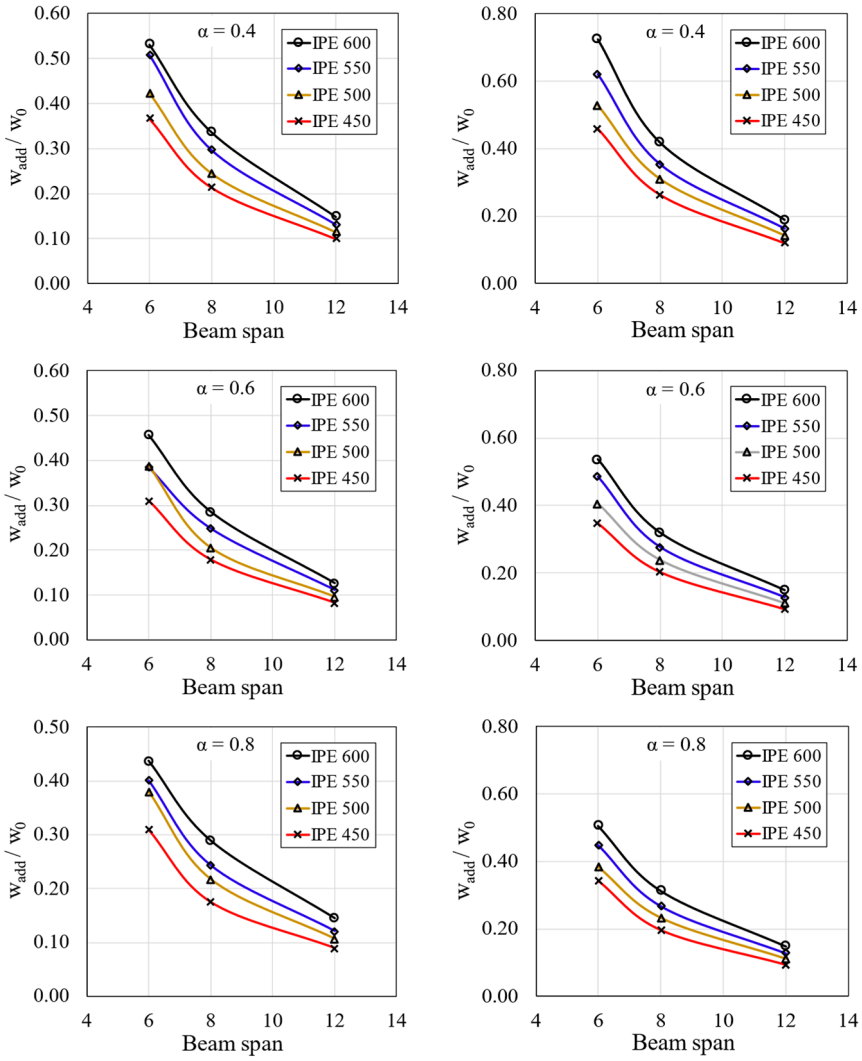
4.2. Influence of Additional Deflection on Unperforated Tapered Steel Beam

It is important to highlight from these results that the presence of variable circular openings in web-tapered beams leads to very important deflections. The SCI P355 guidance design mentioned that the contribution of openings in total deflection varies between 12% and 15% of solid beam, whereas the elements studied on this work, this form of openings amplify the deflection of the solid tapered beams even more than 30% up to 60% for short beams (6 m) and between 10% and 18% for the longest (12 m) (Figure 11). That can also be seen on Figure 12, where for the same tapered web section α, the additional deflection is very significant for the deeper beam and it decreases as the shallow beam height. Moreover, the difference in the influence of the additional deflection on the unperforated beam keeps the same range for almost all load cases. It is evident that this is why the variation in circular opening along the axis of the beam occurs with the variation in the cross-section of the beam. It is important to define that, according to the final expression of the additional deflection, the bending effect is not neglected, as SCI P355 does. The difference is very obvious for large openings in cellular beams.



(**a**) Three-point bending (**b**) Four-point bending

Figure 11. *Cont.*



(**c**) Five-point bending (**d**) Uniformly distributed load

Figure 11. Analytical deflection ratio (w_{add}/w_0) versus beam span.

The results highlight a clear trend: for all configurations, the ratio w_{add}/w_0 decreases as the span increases. This reduction reflects the fact that the reference global deflection w_0, corresponding to a solid-web beam without openings, increases more rapidly with span than the additional deflection w_{add}, which is localised and primarily associated with the web openings. For instance, in the case of the IPE 600 section under three-point bending with $\alpha = 0.4$, the ratio w_{add}/w_0 decreases from 0.62 to 0.24 as the span increases from 6 m to 12 m. The influence of the α parameter is also significant. When α is low ($\alpha = 0.4$), the reduction in height near the supports leads to a local drop in flexural stiffness, thereby increasing the additional deflection induced by the openings. Figure 12 clearly illustrates this trend, partly due to the larger number of openings generated by a more inclined geometry, which further weakens the beam. It should also be noted that, for the same span and cross-section, a beam with a high number of small-diameter openings exhibits greater additional deflection than a beam with fewer, larger-diameter openings. For example, for an IPE600 beam with a span of 6 m, the configuration with $\alpha = 0.4$ results in an additional deflection w_{add} of 8.002 mm, compared to 6.37 mm for $\alpha = 0.6$ and 6.3 mm for $\alpha = 0.8$. Conversely, as α increases and approaches 1, the beam geometry tends towards a prismatic configuration (i.e., constant cross-section). In the limit $\alpha = 1$, the beam becomes geometrically uniform again, and the results converge towards those of traditional cellular beams with constant inertia. For example, for a 6 m span and a four-point bending scenario with the IPE 500

section, the ratio w_{add}/w_0 decreases from 0.44 for $\alpha = 0.4$, to 0.35 for $\alpha = 0.6$, and to 0.28 for $\alpha = 0.8$. It is also observed that, for a given configuration, stiffer profiles such as IPE 600 show higher values of w_{add}/w_0 than smaller profiles (e.g., IPE 450), since the total reference deflection w_0 is smaller, thereby amplifying the relative contribution of the additional deflection. Finally, the loading type plays a crucial role: concentrated loads (three- or five-point bending) generate localised bending moment peaks that often coincide with perforated zones, locally amplifying deformation. In contrast, a uniformly distributed load induces a smoother stress distribution, resulting in more moderate values of w_{add}/w_0. For example, for $\alpha = 0.6$ and the IPE 550 profile, this ratio is 0.31 under five-point bending, compared to 0.26 for a uniformly distributed load over an 8 m span. These observations confirm that the developed analytical formulation consistently captures the combined effect of longitudinal geometric variation and web openings, while remaining applicable to conventional (prismatic) geometries through a simple adjustment of the α parameter.

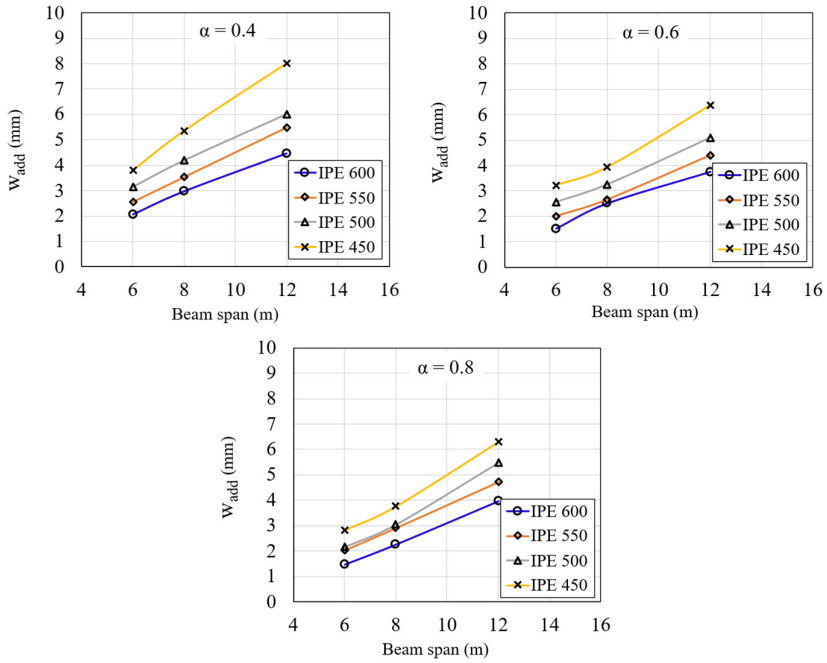


Figure 12. Additional deflection w_{add} versus beam span (IPE600).

5. Conclusions

This study presented an analytical formulation for predicting the additional elastic deflection of tapered steel beams with circular web openings of variable diameter. The main findings and contributions are summarised as follows:

- To the best of the authors' knowledge, the proposed formulation is the first analytical model to simultaneously incorporate cross-section tapering and progressive variation in opening diameter along the span, filling a gap not addressed by any existing analytical model or design code.
- The formulation incorporates a dedicated expression to determine the exact position of each opening, capturing the influence of geometric variation in both the beam profile and the distribution of perforations, significantly extending previous formulations limited to constant-diameter, regularly spaced openings.
- Good overall agreement is observed between the analytical predictions and FEM simulations, with deviations generally below 5% across the full range of configurations investigated. A few isolated cases reach up to +8% for extended spans and −7% for

shorter spans, while under distributed loading conditions, 90% of results remain within a 3% margin.

- For prismatic cellular steel beams, normative approaches such as EC3 and SCI P355 tend to be conservative and exhibit significant inaccuracies in cases involving large openings and short spacing. In contrast, the proposed model delivers more accurate predictions and remains stable and reliable across all studied configurations.
- Tapered beams are more sensitive to the influence of opening diameter on deflection compared to classical cellular beams. Beyond the Vierendeel mechanism, the progressive variation in opening diameter along the span contributes to the amplification of local deformations.
- The method is applicable to both tapered beams with variable-diameter openings and standard prismatic cellular beams, providing a reliable, practical tool for structural engineers to perform accurate and efficient deflection assessments in design applications.

Future research directions:

- Experimental validation of the proposed formulation on tapered steel beams with variable-diameter web openings, once such test data become available in the literature.
- Development of simplified design expressions suitable for direct integration into future design codes.

Author Contributions: Conceptualization, A.O.; Methodology, A.O.; Software, A.O.; Investigation, A.O. and A.K.; Resources, A.Z.; Writing—original draft, A.O.; Writing—review & editing, A.Z., A.K. and S.F.D.; Visualization, S.F.D.; Supervision, S.F.D. All authors have read and agreed to the published version of the manuscript.

Funding: This research received no external funding.

Data Availability Statement: Data is provided within the manuscript.

Conflicts of Interest: The authors declare no conflicts of interest.

Nomenclature

l	Total mid-span deflection of the perforated tapered beam
w_0	Deflection of the unperforated tapered beam (solid web)
w_{add}	Additional deflection due to the presence of circular web openings
$w_{add\ i}$	Additional deflection at opening i
w_t	Deflection of a T-section (upper or lower)
w_{Tb}	Deflection component due to the bending effect in the T-section
w_{Ts}	Deflection component due to the shear effect in the T-section
w_b	Deflection of the unperforated beam (notation from SCI P355)
δ_{add}	Additional deflection (EC3 notation)
δ_b	Deflection of the unperforated beam (EC3 notation)
w_{FEM}	Deflection calculated using the finite element method
w_{EC3}	Deflection calculated according to Eurocode 3
$w_{SCI\ P355}$	Deflection calculated according to the SCI P355 guide
α	Tapered Section parameter
h_{max}, h_m	Total section height at mid-span
h_{min}, h_0	Total section height at the ends
$h(x)$	Total section height at position x
$h_w(x)$	Web height at position x
L	Span of the beam
$A_w(x)$	Aire de l'âme réduite de la section en T à la position x
$d_w(x)$	Distance entre le centroïde de la section en I et celui de l'âme en T à x
$\omega(x)$	Shear area of the T-section at position x
$D(x)$	Diameter of the circular opening at position x
D_0	Initial diameter of the smallest opening
$R(x)$	Radius of the circular opening at position x
R_0	Radius of the first opening (i = 0)
ρ	Diameter-to-total-height ratio, constant along the beam
n	Number of circular openings in the beam
m	Maximum index in the algorithm loop
i	Position index of the opening in the algorithm
x_i	Longitudinal position of the i-th opening
W	Width of the web post between two openings
ψ	Common ratio of the geometric sequence of radii
β	Local plasticization angle around the opening
l	Equivalent length of the Vierendeel lever arm
v	Poisson's ratio
V	Shear force applied to the T-section
n_0	Number of regular openings (EC3 and SCI P355)
k_0	Correction factor according to the type of opening (reinforced or not)
a_0	Width of the opening, EC3 notation
h_0	Height of the opening—EC3/SCI P355 notation
h	Beam height—EC3/SCI P355 notation

t_w	Web thickness	Δ_1	Relative error of the proposed analytical method compared to FEM
t_f	Flange thickness	Δ_2	Relative error of Eurocode 3 compared to FEM
b_f	Flange width	Δ_3	Relative error of SCI P355 compared to FEM
i_f	Moment of inertia of the flange of the T-section	U_x	Longitudinal displacement (x-direction)
i_w	Moment of inertia of the web of the T-section	U_y	Transverse displacement (y-direction)
i_T	Total moment of inertia of the T-section	U_z	Lateral displacement (z-direction)
A_f	Flange area	UR_x	Rotation about the longitudinal x-axis
d_f	Distance between the centroid of the I-section and that of the flange	G	Shear modulus of steel
E	Elastic modulus of steel		

References

1. *EN 1993-1-1:2015*; Recommandations de la CNC2M Pour l'Eurocode 3. BNCM-CNC2M: Paris, France, 2015.
2. Lawson, R.M.; Hicks, S.J. *Design of Composite Beams with Large Web Openings*; Steel Construction Institute: Ascot, UK, 2011.
3. Osmani, A.; Shamass, R.; Tsavdaridis, K.D.; Ferreira, F.P.V.; Khatir, A. Deflection Predictions of Tapered Cellular Steel Beams Using Analytical Models and an Artificial Neural Network. *Buildings* **2025**, *15*, 992. [CrossRef]
4. Zaarour, W.; Redwood, R. Web Buckling in Thin Webbed Castellated Beams. *J. Struct. Eng.* **1996**, *122*, 860–866. [CrossRef]
5. Das, P.K.; Seimaini, S.L. *Handbook for the Design of Castellated Beams*; Abacus Press: Tunbridge Wells, UK, 1984.
6. Zeytinci, B.M.; Şahin, M.; Güler, M.A.; Tsavdaridis, K.D. A practical design formulation for perforated beams with openings strengthened with ring type stiffeners subject to Vierendeel actions. *J. Build. Eng.* **2021**, *43*, 102915. [CrossRef]
7. Degtyarev, V.V.; Tsavdaridis, K.D. Buckling and ultimate load prediction models for perforated steel beams using machine learning algorithms. *J. Build. Eng.* **2022**, *51*, 104316. [CrossRef]
8. Altfillisch, M.D.; Cooke, B.R.; Toprac, A.A. An investigation of welded open-web expanded beams. *J. Am. Weld. Soc. Weld. Res. Suppl.* **1957**, 77–88.
9. Redwood, R.G.; McCutcheon, J.O. Beam Tests with Unreinforced Web Openings. *J. Struct. Div.* **1968**, *94*, 1–17. [CrossRef]
10. Kerdal, D.; Nethercot, D.A. Failure modes for castellated beams. *J. Constr. Steel Res.* **1984**, *4*, 295–315. [CrossRef]
11. Aglan, A.A.; Redwood, R.G. Web buckling in castellated beams. *Proc. Inst. Civ. Eng.* **1974**, *57*, 307–320. [CrossRef]
12. Sonck, D.; Belis, J. Lateral-Torsional Buckling Resistance of Castellated Beams. *J. Struct. Eng.* **2017**, *143*, 04016197. [CrossRef]
13. Boissonnade, N.; Nseir, J.; Lo, M.; Somja, H. Design of cellular beams against lateral torsional buckling. *Proc. Inst. Civ. Eng. Struct. Build.* **2014**, *167*, 436–444. [CrossRef]
14. Panedpojaman, P.; Sae-Long, W.; Chub-Uppakarn, T. Cellular beam design for resistance to inelastic lateral-torsional buckling. *Thin Walled Struct.* **2016**, *99*, 182–194. [CrossRef]
15. de Carvalho, A.S.; de Oliveira, V.M.; Rossi, A.; Martins, C.H. Elastic lateral-torsional buckling behavior of steel I-beams with sinusoidal web openings. *Structures* **2023**, *47*, 23–36. [CrossRef]
16. Tsavdaridis, K.D. *Structural Performance of Perforated Steel Beams with Novel Web Openings and with Partial Concrete Encasement*; Imperial College London: London, UK, 2010.
17. Tsavdaridis, K.D.; D'Mello, C. *Perforated Structural Beams*; Imperial College London: London, UK, 2011.
18. Tsavdaridis, K.D.; D'Mello, C. Web buckling study of the behaviour and strength of perforated steel beams with different novel web opening shapes. *J. Constr. Steel Res.* **2011**, *67*, 1605–1620. [CrossRef]
19. Tsavdaridis, K.D.; D'Mello, C. Optimisation of novel elliptically-based web opening shapes of perforated steel beams. *J. Constr. Steel Res.* **2012**, *76*, 39–53. [CrossRef]
20. Tsavdaridis, K.D.; D'Mello, C. Vierendeel Bending Study of Perforated Steel Beams with Various Novel Web Opening Shapes through Nonlinear Finite-Element Analyses. *J. Struct. Eng.* **2012**, *138*, 1214–1230. [CrossRef]
21. Tsavdaridis, K.D. Applications of topology optimization in structural engineering: High-rise buildings and steel components. *Jordan J. Civ. Eng.* **2015**, *9*, 335–357. [CrossRef]
22. Benyamina, A.B.; Meftah, S.A.; Mohri, F.; Daya, E.M. Analytical solutions attempt for lateral torsional buckling of doubly symmetric web-tapered I-beams. *Eng. Struct.* **2013**, *56*, 1207–1219. [CrossRef]
23. Osmani, A.; Meftah, S.A. Lateral buckling of tapered thin walled bi-symmetric beams under combined axial and bending loads with shear deformations allowed. *Eng. Struct.* **2018**, *165*, 76–87. [CrossRef]
24. Lee, L.H. Non-uniform torsion of tapered i-beams. *J. Frankl. Inst.* **1956**, *262*, 37–44. [CrossRef]
25. Andrade, A.; Camotim, D. Lateral–Torsional Buckling of Singly Symmetric Tapered Beams: Theory and Applications. *J. Eng. Mech.* **2005**, *131*, 586–597. [CrossRef]
26. Zhang, L.; Tong, G.S. Lateral buckling of web-tapered I-beams: A new theory. *J. Constr. Steel Res.* **2008**, *64*, 1379–1393. [CrossRef]
27. Asgarian, B.; Soltani, M.; Mohri, F. Lateral-torsional buckling of tapered thin-walled beams with arbitrary cross-sections. *Thin Walled Struct.* **2013**, *62*, 96–108. [CrossRef]

28. Mohri, F.; Meftah, S.A.; Damil, N. A large torsion beam finite element model for tapered thin-walled open cross sections beams. *Eng. Struct.* **2015**, *99*, 132–148. [CrossRef]
29. Wang, Y.; Chen, B.; Wang, J.; Luo, L.; Li, B.; Ye, Q.; Hai, L. Effect of web openings on the patch loading resistance of QN 1803 high-strength stainless steel plate girders. *Thin Walled Struct.* **2025**, *210*, 113065. [CrossRef]
30. ArcelorMittal. *ACB® and Angelina® Beams: A New Generation of Beams with Large Web Openings*; ArcelorMittal: Luxembourg, 2020.
31. Gibson, E.; Jenkins, W.M. An Investigation of the Stresses and Deflections in Castellated Beams. *Struct. Eng.* **1957**, *35*, 467–479.
32. Iverson, P.A. Some Aspects of the Finite Element Method in Two-Dimensional Problems. In *Finite Element Methods in Stress Analysis*; Tapir-Trykk: Trondheim, Norway, 1969.
33. Hosain, M.U.; Cheng, W.K.; Neis, V.V. Deflection analysis of expanded open-web steel beams. *Comput. Struct.* **1974**, *4*, 327–336. [CrossRef]
34. Lawson, R.M. *Design for Openings in the Webs of Composite Beams*; Steel Construction Institute: Ascot, UK, 1987.
35. Chung, K.F.; Lawson, R.M. Simplified design of composite beams with large web openings to Eurocode 4. *J. Constr. Steel Res.* **2001**, *57*, 135–164. [CrossRef]
36. Lawson, R.M.; Lim, J.; Hicks, S.J.; Simms, W.I. Design of composite asymmetric cellular beams and beams with large web openings. *J. Constr. Steel Res.* **2006**, *62*, 614–629. [CrossRef]
37. Liu, T.C.H.; Chung, H.F. Practical design of Universal steel beams with single web openings of different shapes. In Proceedings of the Second European Conference on Steel Structures, Eurosteel '99, Prague, Czech Republic, 26–29 May 1999; pp. 59–62.
38. *BS 5950-3.1:1990*; Structural Use of Steelwork in Building—Part 3. British Standards Institution: London, UK, 1985.
39. Warren, J.J. Ultimate Load and Deflection Behaviour of Cellular Beams. Master's Thesis, University of Natal, Durban, South Africa, 2001.
40. Djebli, B.; Kerdal, D.E.; Abidelah, A. The Total Deflection of Composite Cellular Beams Under Transverse Loading. *Arab. J. Sci. Eng.* **2014**, *39*, 6815–6824. [CrossRef]
41. Djebli, B.; Kerdal, D.E.; Abidelah, A. Additional and total deflection of composite symmetric cellular beams. *J. Constr. Steel Res.* **2019**, *158*, 99–106. [CrossRef]
42. Sarfarazi, S.; Shamass, R.; Rabi, M.; Abarkan, I.; Ferreira, F.P.V.; Tsavdaridis, K.D. Inverse machine learning for the design of perforated beams: Parent section and material prediction. *Eng. Appl. Artif. Intell.* **2026**, *164*, 113275. [CrossRef]
43. Fang, Z.; Roy, K.; Padiyara, S.; Chen, B.; Raftery, G.M.; Lim, J.B.P. Web crippling design of cold-formed stainless steel channels under interior-two-flange loading condition using deep belief network. *Structures* **2023**, *47*, 1967–1990. [CrossRef]
44. Liu, T.C.H.; Chung, K.F. Steel beams with large web openings of various shapes and sizes: Finite element investigation. *J. Constr. Steel Res.* **2003**, *59*, 1159–1176. [CrossRef]
45. The MathWorks. *MATLAB: The Language of Technical Computing*; The MathWorks: Natick, MA, USA, 2001.
46. Systèmes Dassault. *Abaqus 2017 Online Documentation*; Dassault Systèmes: Vélizy-Villacoublay, France, 2017.
47. Grilo, L.F.; Fakury, R.H.; de Castro e Silva, A.L.R.; de Souza Veríssimo, G. Design procedure for the web-post buckling of steel cellular beams. *J. Constr. Steel Res.* **2018**, *148*, 525–541. [CrossRef]
48. Ferreira, F.P.V.; Rossi, A.; Martins, C.H. Lateral-torsional buckling of cellular beams according to the possible updating of EC3. *J. Constr. Steel Res.* **2019**, *153*, 222–242. [CrossRef]
49. Ferreira, F.P.V.; Martins, C.H. LRFD for Lateral-Torsional Buckling Resistance of Cellular Beams. *Int. J. Civ. Eng.* **2020**, *18*, 303–323. [CrossRef]
50. Rossi, A.; Ferreira, F.P.V.; Martins, C.H.; Mesacasa, E.C., Jr. Assessment of lateral distortional buckling resistance in welded I-beams. *J. Constr. Steel Res.* **2020**, *166*, 105924. [CrossRef]
51. Ferreira, F.P.V.; Shamass, R.; Santos, L.F.P.; Limbachiya, V.; Tsavdaridis, K.D. EC3 design of web-post buckling resistance for perforated steel beams with elliptically-based web openings. *Thin Walled Struct.* **2022**, *175*, 109196. [CrossRef]
52. Ferreira, F.P.V.; Shamass, R.; Santos, L.F.P.; Tsavdaridis, K.D.; Limbachiya, V. Web-post buckling resistance calculation of perforated high-strength steel beams with elliptically-based web openings for EC3. *Structures* **2023**, *55*, 245–262. [CrossRef]

Disclaimer/Publisher's Note: The statements, opinions and data contained in all publications are solely those of the individual author(s) and contributor(s) and not of MDPI and/or the editor(s). MDPI and/or the editor(s) disclaim responsibility for any injury to people or property resulting from any ideas, methods, instructions or products referred to in the content.